AIP Journal of Applied Physics

Optical studies of InN epilayers on Si substrates with different buffer layers

M. D. Yang, J. L. Shen, M. C. Chen, C. C. Chiang, S. M. Lan, T. N. Yang, M. H. Lo, H. C. Kuo, T. C. Lu, P. J. Huang, S. C. Hung, G. C. Chi, and W. C. Chou

Citation: Journal of Applied Physics **102**, 113514 (2007); doi: 10.1063/1.2817826
View online: http://dx.doi.org/10.1063/1.2817826
View Table of Contents: http://scitation.aip.org/content/aip/journal/jap/102/11?ver=pdfcov
Published by the AIP Publishing

Articles you may be interested in
InGaN/GaN multiple-quantum-well light-emitting diodes grown on Si(111) substrates with ZrB2(0001) buffer layers
J. Appl. Phys. **111**, 033107 (2012); 10.1063/1.3684557

Influence of crystal quality of underlying GaN buffer on the formation and optical properties of InGaN/GaN quantum dots
Appl. Phys. Lett. **95**, 101909 (2009); 10.1063/1.3224897

Real time optical monitoring of molecular beam epitaxy of InN on SiC substrates
J. Vac. Sci. Technol. B **25**, 1014 (2007); 10.1116/1.2737433

Cubic InN growth on sapphire (0001) using cubic indium oxide as buffer layer
Appl. Phys. Lett. **90**, 091901 (2007); 10.1063/1.2696282

Spectroscopic ellipsometry study of wurtzite InN epitaxial films on Si(111) with varied carrier concentrations
Appl. Phys. Lett. **86**, 201905 (2005); 10.1063/1.1929097

Re-register for Table of Content Alerts

Create a profile.
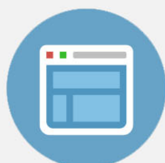
Sign up today!

[This article is copyrighted as indicated in the article. Reuse of AIP content is subject to the terms at: http://scitation.aip.org/termsconditions. Downloaded to] IP: 140.113.38.11 On: Thu, 01 May 2014 00:02:26

Optical studies of InN epilayers on Si substrates with different buffer layers

M. D. Yang and J. L. Shen[a)]
Department of Physics, Chung Yuan Christian University, Chungli, Taoyuan, Taiwan

M. C. Chen, C. C. Chiang, S. M. Lan, and T. N. Yang
Institute of Nuclear Energy Research, Longtan, Taoyuan, Taiwan

M. H. Lo, H. C. Kuo, and T. C. Lu
Department of Photonics and Institute of Electro-Optical Engineering, National Chiao Tung University, Hsinchu, Taiwan

P. J. Huang, S. C. Hung, and G. C. Chi
Department of Physics, National Central University, Chungli, Taoyuan, Taiwan

W. C. Chou
Department of Electrophysics, National Chiao Tung University, Hsin-Chu, Taiwan

(Received 12 June 2007; accepted 3 October 2007; published online 7 December 2007)

We have investigated the photoluminescence (PL) and time-resolved PL from the InN epilayers grown on Si substrates with different buffer layers. The narrowest value of the full width at half maximum of the PL peak is 52 meV with the AlN/AlGaN/GaN triple buffer layer, which is better than previous reports on similar InN epilayers on Si substrates. Based on the emission-energy dependence of the PL decays, the localization energy of carriers is also the least for the InN with a triple buffer layer. According to the x-ray diffraction measurements, we suggest that the reduced lattice mismatch between the InN epilayer and the top buffer layer is responsible for improvement of sample quality using the buffer-layer technique. © *2007 American Institute of Physics*. [DOI: 10.1063/1.2817826]

I. INTRODUCTION

The wide band-gap, group-III nitride compounds have recently attracted much attention because of the applications from the ultraviolet to the near infrared region by proper alloying. Among the group-III nitride semiconductors, InN has attracted extensive attention due to its unusual physical properties and potential applications in optoelectronic devices such as light-emitting diodes, lasers, high-speed electronics, and high-efficiency solar cells.[1–3] With the improvement of growth techniques in the past few years, high-quality InN epilayers grown by molecular-beam epitaxy (MBE) and metalorganic vapor phase epitaxy (MOVPE) are now readily available. However, the growth of high-quality InN is still difficult, due to the low dissociation temperature, the high equilibrium vapor pressure of nitrogen, and the lack of suitable lattice-matched substrates. Among various substrates, sapphire has been widely used for the heteroepitaxial growth of InN, even if it has an insulating property and a large lattice mismatch with InN ($\sim$25%). On the other hand, Si(111) can be the best substrate to grow InN because it offers many attractive advantages such as the smaller lattice mismatch ($\sim$8%), good doping properties, and thermal conductivity. If the Si substrate can be utilized in growing high-quality InN, various optoelectronic devices onto Si-based integrated circuits could be developed in the future. The InN epilayers on Si substrates has been grown recently by MBE,[4–8] metalorganic chemical vapor deposition (MOCVD),[9,10] or magnetron sputter deposition.[11] The growth parameters such as the substrate temperature, nitridation temperature, and orientation have been investigated to optimize sample quality.[5,8,10] One way to improve the quality of InN epilayers is to insert the intermediated buffer layers between the substrate and InN epilayers. Different types of buffer layers, such as the low-temperature InN,[9] GaN,[9] AlN,[4,8,10] and the AlN/Si_3N_4 double layer,[6,7] have been found to be critical parameters to grow high-quality InN epilayers. In this work we performed a study on the photoluminescence (PL) properties of the InN epilayers grown on Si substrates with different buffer layers. As a result of these investigations, we found that the best quality of InN epilayers on a Si substrate is obtained using the AlN/AlGaN/GaN triple buffer layer.

[a)]Author to whom correspondence should be addressed. Electronic mail: jlshen@cycu.edu.tw.

II. EXPERIMENT

The InN epilayers were grown by a home-made atmospheric pressure MOCVD system with a vertical reactor. The liquid MO compounds of trimethyl gallium (TMG), trimethyl amine (TMA), trimethyl indium (TMI), and gaseous NH_3 were employed as the reactant source materials for Ga, Al, In, and N, respectively, and H_2 was used as the carrier gas. The substrate used in this experiment was cut from a (111)-oriented Si wafer. These wafers show *n*-type conductivity with a carrier concentration of around 10^{17} cm^{-3}. Prior to growth, the Si (111) substrate was etched by boiling it in $H_2SO_4:H_2O_2=3:1$ for 15 min and then dipped in a Hartree–Fock (HF) solution (HF: $H_2O=1:10$) for 15 s to remove native oxide formed on the surface. For the triple buffer layer

 © 2007 American Institute of Physics

[This article is copyrighted as indicated in the article. Reuse of AIP content is subject to the terms at: http://scitation.aip.org/termsconditions. Downloaded to] IP: 140.113.38.11 On: Thu, 01 May 2014 00:02:26

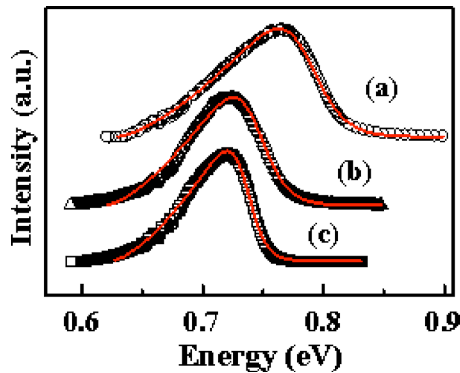

FIG. 1. (Color online) Measured (circles) and calculated (solid line) PL of the three InN samples with different buffer layers: (a) AlN single buffer layer (sample A); (b) AlN/GaN double buffer layer (sample B); (c) AlN/AlGaN/GaN triple buffer layer (sample C).

sample (sample C), the AlN, AlGaN, and GaN were grown in sequence at 1130 °C for a total growth time of 18 min using a TMA flow of 23 sccm, a TMG flow of 5 sccm, and a NH_3 flow of 2.74 slm, respectively. For the double (single) buffer layer sample, only the AlN/GaN (AlN) buffer layers were grown, which has been assigned as sample B (sample A). Finally, the low- and high-temperature epitaxy InN layers with a total thickness of approximately 230 nm were grown at 440 and 620 °C, respectively.

The PL measurements were obtained using a diode laser operating at a wavelength of 976 nm as the excitation source. The collected luminescence was directly projected into a grating spectrometer and detected with an extended InGaAs detector. The diode laser produces light pulses with 50 ps duration and a repetition rate of 1 MHz. The PL decay signals were measured using the technique of time-correlated single-photon counting. The overall temporal response function of the system is 250 ps.

III. RESULTS AND DISCUSSION

The 10 K PL spectra of the InN epilayers on Si with different buffer layers are shown in Fig. 1. Each spectral shape of the main emission line is asymmetric, having a sharp slope at the high-energy side and a broad tail on the low-energy side of the spectrum. It is found that the full width at half maximum (FWHM) of the PL is 79, 61, and 52 meV for the InN epilayers with the AlN single buffer layer (sample A), the AlN/GaN double buffer layer (sample B), and the AlN/AlGaN/GaN triple buffer layer (sample C), respectively. This observation reveals that the quality of InN epilayers can be greatly improved by using the AlN/AlGaN/GaN triple buffer layer in the heteroepitaxial growth of the InN on the Si substrates. The FWHM of the PL peak for the triple buffer layer InN epilayers is better than previous reports on similar InN epilayers on Si substrates.[9,10]

The shape of the PL band can be analyzed according to the following expression:[12]

$$I(\hbar w) \sim [\hbar w - E_g(n)]^{\gamma/2} f(\hbar w - E_g(n) - E_f), \quad (1)$$

where E_f is the Fermi energy, n is the fitting carrier concentration, $E_g(n)$ is a carrier-concentration-dependent band gap, f is the Fermi–Dirac function, and γ is the parameter that

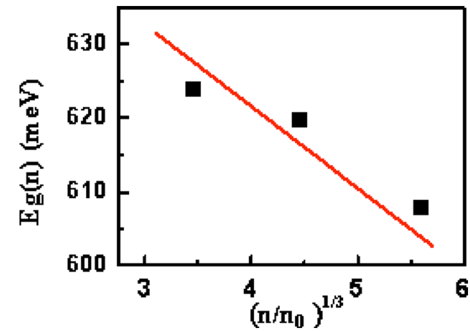

FIG. 2. (Color online) $E_g(n)$ as a function of the carrier concentration for the InN epilayers (closed squares). n_0 is 1×10^{18} cm^{-3}. The solid line is a fitted curve using Eq. (2).

involves the relaxation of the momentum conservation law in the interband transitions.[12] The solid lines in Fig. 1 show the fitted PL spectra of InN with different buffer layers according to Eq. (1), revealing a good agreement between the fitting curves and the experimental data. The closed squares in Fig. 2 show the parameter $E_g(n)$ as a function of the carrier concentration. It reveals a nearly linear dependence on $n^{1/3}$, in agreement with the previous result.[12] This empirical relation can be described by the following expression:

$$E_g(n) = -11.1(n/10^{18})^{1/3} + 0.666, \quad (2)$$

plotted as a solid line in Fig. 2. By extrapolating $E_g(n)$ to the limit electron concentration, we obtain a band-gap energy of 0.666 eV for intrinsic InN. This value is within the range of the band-gap value of 0.6–0.8 eV in recent reports.[13–16]

The carrier concentrations of the InN samples with different buffer layers were obtained from the Hall-effect measurements at room temperature. The carrier concentrations of 1.8×10^{20}, 8.8×10^{19}, and 4.1×10^{19} cm^{-3} were obtained for the InN samples A, B, and C, respectively. The carrier concentrations are decreased monotonously, demonstrating that the quality of the InN epilayers can be improved using the buffer layer technique. Figure 3 displays the PL decay profiles of the InN epilayers with different buffer layers. The PL transient profiles are found to be a single exponential decay and can be fitted by the function $I(t)=I_0 \exp(-t/\tau)$, where τ is the carrier lifetime, one of the crucial indicators of the materials quality. The carrier lifetime increases from sample A to C, in agreement with the Hall-effect measurements and demonstrating again the best quality of our investigated InN epilayers is sample C.

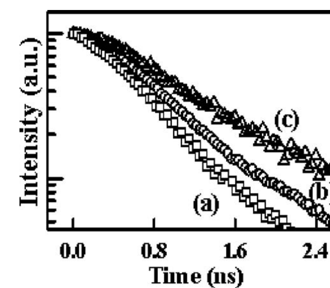

FIG. 3. PL decay profiles of the three InN samples with different buffer layers: (a) sample A; (b) sample B; (c) sample C.

[This article is copyrighted as indicated in the article. Reuse of AIP content is subject to the terms at: http://scitation.aip.org/termsconditions. Downloaded to] IP: 140.113.38.11 On: Thu, 01 May 2014 00:02:26

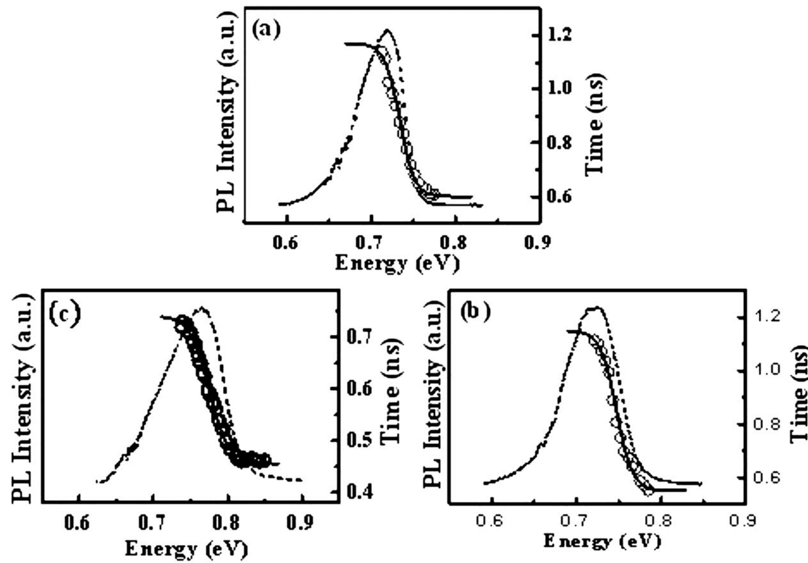

FIG. 4. Emission-energy dependence of lifetime τ (open circles) of three InN samples with different buffer layers: (a) sample A; (b) sample B; (c) sample C. The solid lines display the calculated τ using Eq. (3). The PL spectra of InN are also shown (the dashed lines).

The open circles in Fig. 4 show the emission-energy dependence of lifetime τ for the InN epilayers with different buffer layers. The decrease of the lifetimes with increasing emission energy is a characteristic of the localization effect. The combination of recombination and transfer has been modeled by assuming the density of localized tail states is proportional to $\exp(-E/E_0)$, where E_0 describes the amount of spreading in the density of states.[17,18] The relationship between lifetime $\tau(E)$ and PL energy E can be described by the function[17,18]

$$\tau(E) = \frac{\tau_{\mathrm{rad}}}{1+\exp[(E-E_{me})/E_0]}, \tag{3}$$

where τ_{rad} is the radiative lifetime and E_{me} is defined by a definite energy for which the decay time equals the transfer time. $\tau(E)$ fitted by Eq. (3) are plotted with the solid lines in Fig. 4. The good fits to experiments confirm the existence of carrier localization. E_0 here is a measure of average localization energy in InN. The open squares in Fig. 5 plot E_0 for three InN samples with different buffer layers. E_0 decreases monotonically from sample A to C. Recent studies reveal that carrier localization in InN is associated with the potential fluctuation of the randomly located impurities.[14,15,19] In heavily doped semiconductors such as InN, the inhomogeneous impurity distribution may produce a density-of-state tail by electron-impurity interactions. Such a band tail localizes the photogenerated carriers and can be treated as acceptor-type centers, distributed above the top of the valence band. The localization energy of carriers has been calculated based on the localized holes in the tail states, demonstrating that carrier localization in InN originates from the potential fluctuations of randomly located impurities.[19] Therefore, the decrease of E_0 in Fig. 5 implies that the potential fluctuation of randomly located impurities is reduced from sample A to C.

To investigate the origin of the sample improvement by using the buffer layer technique, the structural properties of the studied InN epilayers were investigated. Figure 6 shows the θ-2θ x-ray diffraction (XRD) spectra of the InN epilayers with different buffer layers. The observed diffraction lines exhibited dominant (0002) α-InN reflection at ~31° for all samples, revealing that the InN epilayers mainly consisted of the hexagonal InN phase. From the observed (0002) diffraction the lattice constant c can be obtained. The inset of Fig. 6 plots the lattice constant c obtained from the XRD for the investigated samples, including a previously reported value of a bulk crystal.[20] Among the three kinds of buffer layers, sample C (sample A) shows the closest (farthest) lattice constant to the value of the bulk crystal. The difference in lattice constant is attributed to the residual strain that remains in the InN, originating from lattice mismatch between the InN ep-

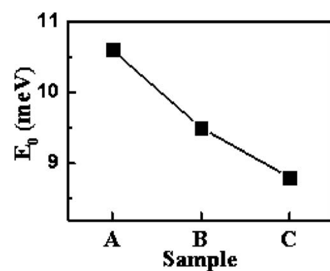

FIG. 5. Localization energy E_0 obtained from Eq. (3) (closed squares) of three samples. The line is a guide to the eye.

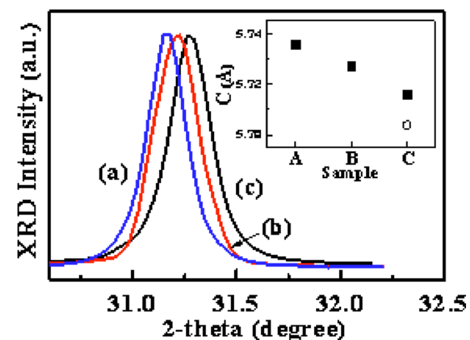

FIG. 6. (Color online) XRD patterns of three InN samples with different buffer layers: (a) sample A; (b) sample B; (c) sample C. Inset: Lattice constant c determined by the XRD for various InN samples (closed squares). The literature value of a bulk InN crystal is given for comparison (open circle).

[This article is copyrighted as indicated in the article. Reuse of AIP content is subject to the terms at: http://scitation.aip.org/termsconditions. Downloaded to] IP: 140.113.38.11 On: Thu, 01 May 2014 00:02:26

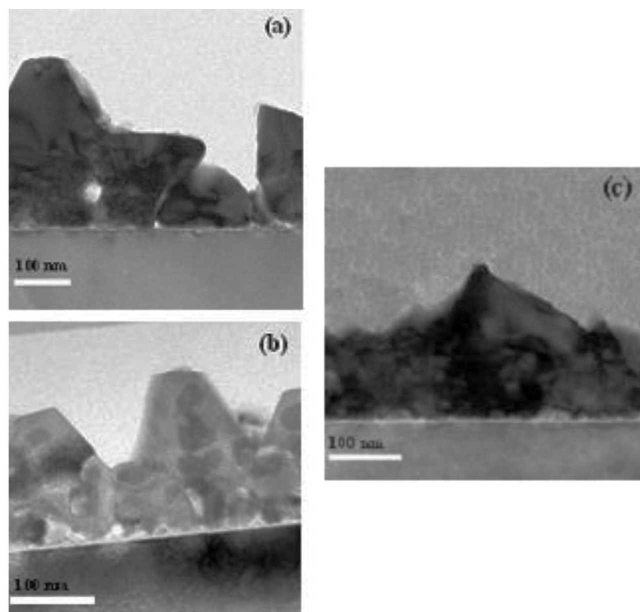

FIG. 7. XTEM images of the three InN samples with different buffer layers: (a) sample A; (b) sample B; (c) sample C.

ilayers and the top buffer layer. It is known that a large lattice mismatch will lead to defects or misfit dislocations in the epilayers. Therefore, better optical properties for sample C are attributed to the lesser lattice mismatch between the InN epilayer and the top buffer layer. Figure 7 shows the cross-sectional transmission electron microscopy (XTEM) images of the InN epilayers with different buffer layers. Irregular cracking or discontinuity of the epilayers can be observed in sample A [Fig. 7(a)]. Sample B exhibits a continuous layer but there are indium clusters visible within the crystal, as reported previously.[21] Sample C has a coalescence layer, and no precipitates or clusters are observed. The results of the XRD and the TEM are thus in good agreement with those results obtained from the PL and time-resolved PL.

IV. SUMMARY

The optical and electrical properties of the InN epilayers on Si with different buffer layers were studied. The narrowest value of the FWHM of the PL peak is 52 meV with the AlN/AlGaN/GaN triple buffer layers, which is smaller than that of the AlN single buffer layer and better than previous reports on similar InN epilayers on Si substrates. In the emission-energy dependence of time-resolved experiments, the depth of the localized states (the potential fluctuation of randomly located impurities) is also smallest for the InN epilayers with the AlN/AlGaN/GaN triple buffer layer. Based on the XRD measurements, we suggest that improvement of the optical properties in the InN epilayers by the AlN/AlGaN/GaN triple buffer layer is attributed to the reduced lattice mismatch between the InN epilayer and the top buffer layer.

ACKNOWLEDGMENTS

The authors are thankful to the Institute of Physics, Academia Sinica, Taiwan for the XRD characterization of the samples. This project was supported by the National Science Council of Taiwan under Grant Nos. NSC 93-2112-M-033-010 and 93-2120-M-033-001, and the Center-of-Excellence Program on Membrane Technology, the Ministry of Education, Taiwan.

[1]A. G. Bhuiyan, A. Hashimoto, and A. Yamamoto, J. Appl. Phys. **94**, 2779 (2003).
[2]K. S. A. Butcher and T. L. Tansley, Superlattices Microstruct. **38**, 1 (2005).
[3]B. Monemar, P. P. Paskov, and A. Kasic, Superlattices Microstruct. **38**, 38 (2005).
[4]F. Agulló-Rueda, E. E. Mendez, B. Bojarczuk, and S. Guha, Solid State Commun. **115**, 19 (2000).
[5]T. Yodo, H. Yona, H. Ando, D. Nosei, and Y. Harada, Appl. Phys. Lett. **80**, 968 (2002).
[6]S. Gwo, C. L. Wu, C. H. Shen, W. H. Chang, T. M. Hsu, J. S. Wang, and J. T. Hsu, Appl. Phys. Lett. **84**, 3765 (2004).
[7]H. Ahn, C. H. Shen, C. L. Wu, and S. Gwo, Appl. Phys. Lett. **86**, 201905 (2005).
[8]J. Grandal and M. A. Sánchez-García, J. Cryst. Growth **278**, 373 (2005).
[9]A. Yamamoto, Y. Yamauchi, M. Ohkubo, A. Hashimoto, and T. Saitoh, Solid-State Electron. **41**, 149 (1997).
[10]B. Maleyre, S. Ruffenach, O. Briot, B. Gil, and A. Van der Lee, Superlattices Microstruct. **36**, 517 (2004).
[11]T. J. Kistenmacher and W. A. Bryden, Appl. Phys. Lett. **59**, 1844 (1991).
[12]V. Yu. Davydov, A. A. Klochikhin, V. V. Emtsev, D. A. Kurdyukov, S. V. Ivanov, V. A. Vekshin, F. Bechstedt, J. Furthmuller, F. Aderhold, J. Graul, A. V. Mudryi, H. Harima, A. Hashimoto, A. Yamamoto, and E. E. Haller, Phys. Status Solidi B **234**, 787 (2002).
[13]M. Higashiwaki and T. Matsui, J. Cryst. Growth **269**, 162 (2004).
[14]A. A. Klochikhin, V. Yu. Davydov, V. V. Emtsev, A. V. Sakharov, V. A. Kapitonov, B. A. Andreev, H. Lu, and W. J. Schaff, Phys. Rev. B **71**, 195207 (2005).
[15]B. Arnaudov, T. Paskova, P. P. Paskov, B. Magnusson, E. Valcheva, B. Monemar, H. Lu, W. J. Schaff, H. Amano, and I. Akasaki, Phys. Rev. B **69**, 115216 (2004).
[16]G. W. Shu, P. F. Wu, Y. W. Liu, J. S. Wang, J. L. Shen, T. Y. Lin, P. J. Pong, G. C. Chi, H. J. Chang, Y. F. Chen, and Y. C. Lee, J. Phys.: Condens. Matter **18**, L543 (2006).
[17]T. Passow, K. Leonardi, H. Heinke, D. Hommel, D. Litvinov, A. Rosenauer, D. Gerthsen, D. Litvinov, A. Rosenauer, D. Gerthsen, J. Seufert, G. Bacher, and A. Forchel, J. Appl. Phys. **92**, 6546 (2002).
[18]M. Strassburg, M. Dworzak, H. Born, R. Heitz, A. Hoffmann, M. Barteis, K. Lischka, D. Schikora, and J. Christen, Appl. Phys. Lett. **80**, 473 (2002).
[19]G. W. Shu, P. F. Wu, M. H. Lo, J. L. Shen, T. Y. Lin, H. J. Chang, Y. F. Chen, C. F. Shih, C. A. Chang, and N. C. Chen, Appl. Phys. Lett. **89**, 131913 (2006).
[20]W. Paszkowicz, R. Cerny, and S. Krukowski, Powder Diffr. **18**, 114 (2003).
[21]J. C. Ho, P. Specht, Q. Yang, X. Xu, D. Hao, and E. R. Wober, J. Appl. Phys. **98**, 093712 (2005).

[This article is copyrighted as indicated in the article. Reuse of AIP content is subject to the terms at: http://scitation.aip.org/termsconditions. Downloaded to] IP: 140.113.38.11 On: Thu, 01 May 2014 00:02:26